UPGRADED USAGE OF ATMOSPHERIC MOTION VECTORS FROM ALL GEOSTATIONARY SATELLITES IN THE OPERATIONAL GLOBAL AND MESO-SCALE 4D-VAR ASSIMILATION SYSTEM AT JMA

Koji Yamashita

Japan Meteorological Agency (JMA) / Numerical Prediction Division
1-3-4, Otemachi, Chiyoda-ku, Tokyo 100-8122, Japan

Abstract

The usage of Atmospheric Motion Vectors (AMVs) in the BUFR-encoded dataset (BUFR AMVs) generated from all geostationary satellites was revised in the JMA operational global 4D-Var assimilation system on 18 October 2006, and in the JMA operational mesoscale 4D-Var assimilation system on 7 December 2007. This revision included the replacement of SATOB AMVs with BUFR AMVs, the introduction of hourly MTSAT-1R AMVs and improvement of the pre-processing method in both assimilation systems.

Before the revision, BUFR AMVs generated from only METEOSAT satellites and SATOB AMVs from MTSAT-1R and GOES satellites had been assimilated in both systems. BUFR AMVs have a great advantage over SATOB AMVs in their high-density distribution and the availability of quality information known as Quality Indicator (QI). For this reason, all SATOB AMVs were replaced with corresponding BUFR AMVs in both assimilation systems.

We also made several revisions to the pre-processing method in both systems in order to use BUFR AMVs efficiently. Firstly, the usage of data is limited more strictly, reflecting error characteristics according to height. Secondly, fewer but more reliable data selected through a more rigorous QI threshold are assimilated. Lastly, a new intelligent thinning scheme was introduced to select only one instance of wind in a thinning box of every 2 degrees in horizontal and 100 hPa in vertical in the six-hour time window, taking into account higher QI values and the proximity to the time of analysis and the centre of the thinning box. This scheme enables the data to be homogeneously distributed.

The revised AMV assimilation scheme reduced the slow bias and Root Mean Square Error (RMSE) of wind speed in analysis fields compared to radiosonde measurements in both assimilation systems. It also improved two-day forecast ability in terms of 250 hPa winds, 500 hPa geopotential heights and 850 hPa temperatures mainly in the southern hemisphere for the global assimilation system. In the mesoscale assimilation experiment with the new AMV scheme, there was an improvement in one-day forecasting for precipitation over 15 mm per three hours around Japan.

We also got a possibility that the thinning interval of AMVs can be reduced from 200 km or 2 degrees in horizontal to bring good impacts on forecast.

1. INTRODUCTION

The operational changes in JMA related to usage of AMVs since 8th International Winds Workshop, held in April 2006, are shown in table 1. The upgraded usage of AMVs using 1-hourly data of MTSAT-1R was implemented to the JMA operational global 4D-Var data assimilation system (GSM-DA) on 18 October 2006 (Yamashita, 2007), and to the JMA operational mesoscale 4D-Var data assimilation system (MSM-DA) on 7 December 2007. Background for upgraded usage of AMVs is as follows.

First, BUFR AMVs have a great advantage over SATOB AMVs in the quality and quantity. Before the revision, BUFR AMVs generated from only two METEOSAT satellites and SATOB AMVs generated from MTSAT-1R and two GOES satellites had been assimilated in both GSM-DA and MSM-DA systems. Advantage of BUFR AMVs over SATOB AMVs is the high-density distribution and the availability of quality information known as QI. Assimilating rapid scan GMS5 AMVs over QI=80 in global 3D-Var assimilation system brought reducing typhoon forecast errors until two-day forecasts

(Nakamura *et al.*, 2002). Assimilating hourly GOES9 AMVs over QI=70 in mesoscale 4D-Var assimilation system brought the better rainfall forecast over the Japan Island (Sato and Kumabe, 2004). Assimilating hourly MTSAT-1R AMVs using the QI thresholds for METEOSAT (Table 2) in MSM-DA system brought a better analysis by deepening trough over eastern China and those results gave a better precipitation forecast in the vicinity of Japan (Yamashita, 2006). Based on these results, we decided to use BUFR AMVs including hourly AMVs. And the revision of usage of AMVs including QI threshold was implemented.

The second is migration to Table-driven Code Forms in the Fourteens WMO Congress (Cg-XIV), held in 2003. We had to use the BUFR AMVs instead of SATOB AMVs.

The third is improvement in thinning scheme. The detail is shown in Section 3(D).

This report describes the upgraded usages of AMVs, as follows. The next Section describes about JMA operational data assimilation and forecast systems briefly. The third Section explains the upgraded usage of AMVs. The fourth and fifth Sections show the experimental results of the new AMV scheme in both assimilation systems. And then, the sixth Section introduces the topics in the experimental results of MSM-DA.

DATE/MONTH/YEAR	EVENT
14/06/2006	Switch from Meteosat-7 to Meteosat-8 BUFR winds.
21/06/2006	Switch from GOES-10 to GOES-11 SATOB winds.
18/10/2006	Upgraded usage of AMVs in GSM-DA (T106L40 (120 km)). Switch from GOES-11/12, MTSAT-1R SATOB to BUFR. Start using MTSAT-1R hourly winds.
05/02/2007	Switch from Meteosat-5 to Meteosat-7 BUFR winds.
24/04/2007	Switch from Meteosat-8 to Meteosat-9 BUFR winds.
21/11/2007	Global forecast model upgrading from TL319L40 (60 km) to TL959L60 (20 km). 4D-Var inner resolution upgrading FROM T106L40 (120 km) to T159L60 (80 km).
07/12/2007	Upgraded usage of AMVs in MSM-DA.
25/03/2008	Start using MTSAT-1R IR4 winds in GSM-DA and MSM-DA.

Table 1: The operational changes related to AMVs since 8th International Winds Workshop in April 2006. explanatory note: T106L40 is truncation wave number of triangular 106 by quadratic grid, corresponding to around 120 km in the horizontal resolution, and vertical layer 40. TL319L40 is truncation wave number of triangular 319 by liner grid and vertical layer 40.

QI threshold	Extra-tropical (x>=20° or x<=-20°)	Tropical （-20° <x<20°)
IR : high level < 400 hPa	60	85
IR : middle level (400 hPa < x <= 700 hPa)	60	60
IR : low level > 700 hPa	75	70
VIS : only low level	60	60
WV : only high level	90	70

Table 2: QI threshold for METEOSAT-5 and METEOSAT-7 until 18 October 2006 (citation from Yamashita, 2006).

2. DATA ASSIMILATION AND FORECAST SYSTEM AT JMA

JMA has the operational global spectral model (JMAGSM) for one-week forecast, short-range forecast and aeronautical forecast, and the operational mesoscale model (JMAMSM) for the purpose of warning for disaster.

JMAGSM is a hydrostatic spectral model with resolution of 20 km (inner-loop model for GSM-DA is 80 km.) in horizontal and 60 vertical levels up to 0.1hPa. In the operational GSM-DA, 6-hourly continuous data assimilation is performed with 6-hour window. The observation data is treated as about one-hour time resolution in the operational GSM-DA. Global forecasts are performed for 216 hours (Fig.1).

JMAMSM is a non-hydrostatic grid model with a horizontal resolution of 5 km and 50 vertical levels up to about 21800 meters. JMAMSM for MSM-DA (JMAMSM-DA) is a hydrostatic spectral model with resolution of 10 km (inner-loop model is 20 km.) in horizontal and 40 vertical levels up to 10 hPa. JMAMSM-DA provides first-guess for quality control (QC). It covers the Japan islands and its surrounding region with the extent of 3600 km by 2880 km. The domain is shown in Fig.2. In the

operational MSM-DA, 3-hourly continuous data assimilation is performed with 6-hour window. The observation data is treated as one-hour time resolution in the operational MSM-DA. To rescue the data delaying from the short data cut-off time (fifty minutes from analysis time), MSM-DA has overlap of 3-hour window. Mesoscale forecasts (15-hour or 33-hour) are performed (Fig.2).

3. REVISED USAGE OF AMVS

(A) NEW DATA

JMA has been using hourly MTSAT-1R AMVs generated from JMA/MSC (Imai, 2006) since 18 October 2006 in GSM-DA and since 7 December 2007 in MSM-DA.

(B) BLACKLISTING IN SPACE

Before the revision, all IR AMVs (700-1000 hPa) below 1.5 m/s wind speed were blacklisted and removed. We investigated the error characteristics according to height using the departure of AMVs observations from the first-guess (O-B) from March 2006 to May 2006. First guess was taken from JMAGSM and JMAMSM-DA. We found that large errors in O-B were not able to be removed by the following QI screening and decided to implement a stricter and finer blacklist check, shown in Fig.3. Difference between GSM-DA and MSM-DA is mainly the usage of mid level AMVs. MSM-DA uses the mid level AMVs of MTSAT-1R but GSM-DA does not use. Because accuracy of the all mid level AMVs recently has become better, we plan to use them in GSM-DA too.

(C) QI THRESHOLDS

Before the revision, JMA had used QI generated from only METEOSAT satellites to screen bad quality data (Yamashita, 2006; Table 2).

To use the QI generated from all geostationary meteorological satellite, we investigated statistical relation between QI and O-B Standard Deviation (SD), biases. It confirmed that the larger QI the smaller O-B SD and bias. Then, the QI thresholds were decided from O-B SD of all QI values over 60 taking into account biases (Table 3). Criteria of O-B SD is 5 m/s for HL, 4 m/s for ML, 2 m/s for LL. Bias below 2 m/s was accepted. These tables are characterised by large QI values in the extra tropical region and in the high level winds.
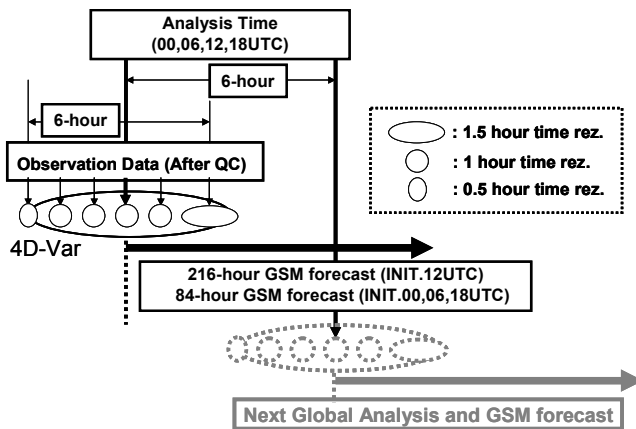
Figure 1: Process flow of JMA operational Global Analysis and JMAGSM forecast

(D) THINNING SCHEME

A thinning procedure is important for
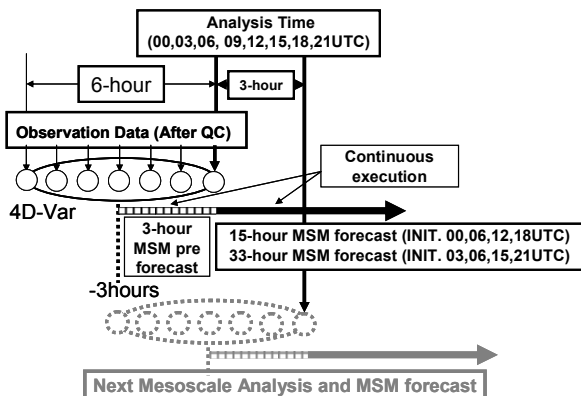
Figure 2: Process flow of JMA operational Mesoscale Analysis and MSM forecast (left side figure), and domain of JMAMSM (right side figure). Kyushu area is framed by an orange line and Chubu by green.

removing redundant AMV data and for reducing computer burden and for avoiding effect of spatial correlation of observation errors. JMA 4D-Var systems don't assume spatial correlation of observation errors to reduce the computation. JMA had used a reported-order thinning method (Yamashita, 2006). This method was simple, but caused a highly inhomogeneous distribution (Fig.4b). For example, comparing Fig.4a and Fig.4b, the observation information can be lost over south-east-sea of Japan in Fig.4b. To avoid them, JMA upgraded the thinning scheme to the equal-distance (Fig. 4c). In this new method, first, AMVs are thinned in a thinning box of every 2 degrees in horizontal and 100 hPa in vertical. A minimum horizontal distance is 200 km. Criteria for selecting an AMV is minimum value of equation taking into account larger QI values and the proximity to the time of analysis and the center of the thinning box in each grid box. The equation is as follows.

$$Tq = \left(\omega_1 \frac{\alpha}{180_{min.}} + \omega_2 \frac{\beta}{2^{\circ}} + \omega_3 \frac{\gamma}{100} \right) \times 100 \quad (1)$$

Tq: Total quality value α : Difference time from time of analysis (unit: minute)
β : Distance from the center of the thinning box (unit: degree) γ : 100 – QI
ω_1=6 ω_2 = ω_3=2

Finally, one AMV per box is selected in a six-hour time window. If the distance between neighboring AMVs is shorter than 200 km, the AMV with the lowest Tq is selected. In addition, the equal-distance thinning scheme in a thinning box of every 1.5degrees in horizontal and 100 hPa in vertical have been applied to Terra CIMSS MODIS and Aqua CIMSS MODIS polar AMVs in the Arctic since 27 May 2004 (Kazumori and Nakamura, 2004). But the thinning scheme of MODIS AMVs is not taking into account QI. We will revise usage of MODIS AMVs in March 2009.

What is the basis of the horizontal size of the thinning box? We investigated the distance dependency of correlation of departure between MTSAT-1R AMV and radiosonde observations (AMV-radiosonde) using Hollingworth-Lönnberg method (Hollingsworth and Lönnberg, 1986). Only Japanese radiosonde observation from March 1, 2006 to May 28, 2007 were used in this study. This result showed statistically slight spatial correlation of observation errors for distance up to 200 km (Fig.5). This result showed MTSAT-1R AMVs above 400 hPa had negligible spatial correlation of observation errors beyond 200 km distance between them. In other sensors and other heights, there were not sufficient samples of AMV-radiosonde. We also investigated the distance dependency of correlation of O-B departure between MTSAT-1R AMV and first guess of JMAMSM (the right panel of Fig.5) and obtained the similar result.

Figure 3: Blacklisting in space for GSM-DA and MSM-DA. These are shown in red area. IR is AMV generated from infrared sensor. WV is AMV generated from infrared sensor of water vapor. NH is Northen hemisphere and SH is Sorthen hemisphere.

		extratropics(NH/SH)			tropics		
		HL	ML	LL	HL	ML	LL
Meteosat-7	IR	94/94	94/94	86/85	84	88	85
	VIS	-/-	-/-	-/88	-	-	84
	WV	95/95	-/-	-/-	88	-	-
Meteosat-9	IR	94/90	90/90	80/80	82	88	85
	VIS	-/-	-/-	82/82	-	-	82
	WV	94/94	-/-	-/-	84	-	-
GOES-11/12	IR	60/60	60/60	60/60	60	60	60
	VIS	-/-	-/-	60/60	-	-	60
	WV	60/60	-/-	-/-	60	-	-
MTSAT-1R	IR	98/96	96/94	84/84	84	84	85
	VIS	-/-	-/-	84/84	-	-	84
	WV	95/90	-/-	-/-	88	-	-

(a) QI shresholds for GSM-DA

		HL	ML	LL
MTSAT-1R	IR	95	95	86
	VIS	–	–	86
	WV	96	–	–

(b) QI shresholds for MSM-DA

tropics: 20S-20N
extratropics: NH:polewards of 20N
            SH:polewards of 20S
HL: 10-400 hPa
ML: 400-700 hPa
LL: 700-1000 hPa

Table 3: QI thresholds for GSM-DA and MSM-DA. All value is QI with first guess check. Red area is over QI=90.

(a)   **(b)**   **(c)**
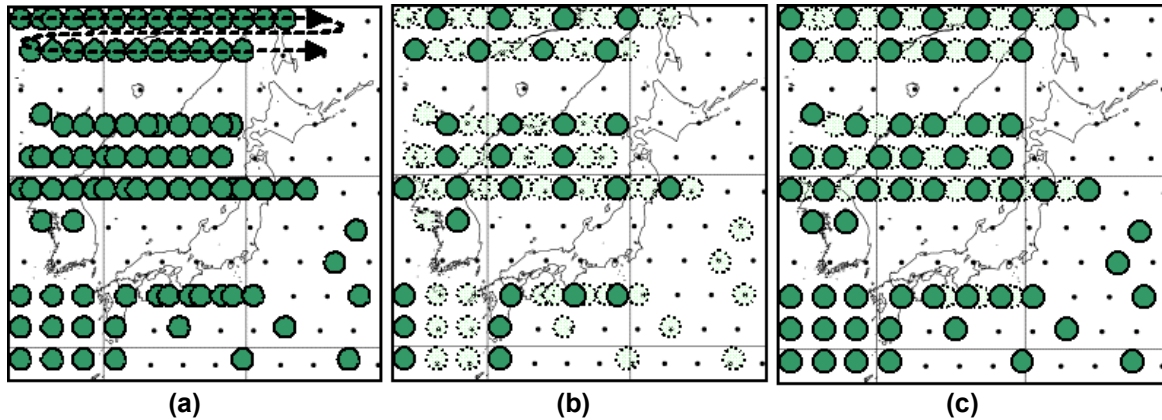
Figure 4: AMV data distributions by one-third thinning of reported-order thinning method (citation from Yamashita 2006).
(a) : AMV data distributions before thinning AMV data. The reported-order AMV data are indicated by arrows.
(b) : AMV data distributions after the one-third thinning of reported-order thinning method.
(c) : AMV data distributions corresponding the one-third thinning by equal-distance thinning method.
Green color circles indicate surviving AMV data positions. Light green color dash circles indicate removing AMV data. Black color dots are grid points.
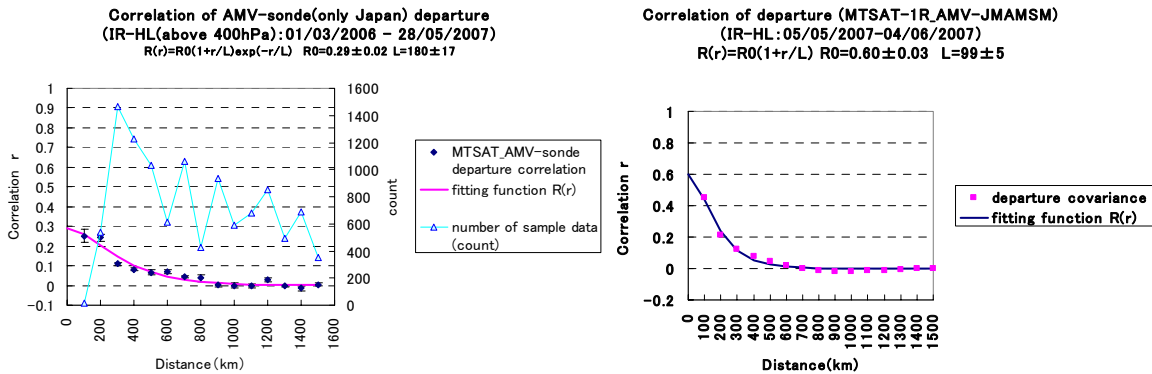
Figure 5: correlation of departure between MTSAT-1R AMV and radiosonde observations (left side figure). The period was from March 1, 2006 to May 28, 2007. And correlation of departure between MTSAT-1R AMV and first guess of JMAMSM (right side figure). The period was from May 5, 2007 to June 4, 2007.

The distance dependency of AMVs from other satellites at various heights estimated using JMAGSM also showed similar results. Therefore, the horizontal size of the thinning box was decided at 200 km or about 2 degree.

4.   OVERVIEW OF EXPERIMENTS

(A) EXPERIMENTAL DESIGN FOR GLOBAL 4D-VAR DATA ASSIMILATION SYSTEM （GSM-DA）

Experiments of GSM-DA were performed to evaluate an impact of the revised usage of AMVs. The data assimilation system is global 4D-Var. The resolution of the system was with 60 km for JMAGSM and 120 km for GSM-DA in horizontal and 40 layers in vertical. Global 4D-VAR data assimilation cycles were run every six hours and 216-hour forecasts were executed only from 12 UTC initial time. Specification of the experiments is as follows.

　　　　Summer experiments) period of GSM-DA: from 00 UTC 24/08/2005 to 18 UTC 09/10/2005
　　　　　　　　　　　　　period of JMAGSM: from 01/09/2005 to 30/09/2005 only 12 UTC
　　　Winter experimets) period of GSM-DA: from 00 UTC 20/12/2005 to 18 UTC 09/02/2006
　　　　　　　　　　　　　period of JMAGSM: from 01/01/2006 to 31/01/2006 only 12 UTC

> CNTL) with BUFR AMVs generated from only METEOSAT5,8 satellites and with SATOB AMVs from MTSAT-1R and GOES10,12 satellites (identical to the operational data)
>> ➢ Using the quality control procedure before the revision (The details are section 3.)
>
> TEST) with BUFR AMVs generated from MTSAT-1R (including hourly AMVs) ,GOES10,12 and METEOSAT5,8 satellites
>> ➢ Using the revised quality control procedure (The details are section 3.)

(B) EXPERIMENTAL DESIGN FOR MESO-SCALE 4D-VAR DATA ASSIMILATION SYSTEM (MSM-DA)

The data assimilation system is 4D-VAR. The MSM-DA cycles were run every three hours and 33-hour or 15-hour forecasts were executed from initial time of 03,09,15,21 UTC, and from 00,06,12,18 UTC, respectively, following the operational implementation. Four experiments were performed in three seasons to assess an impact of new scheme and spatial correlation of observation errors.

> Summer experiment 1: period of MSM-DA: from 00 UTC 07/06/2007 to 21 UTC 13/06/2007
>> period of JMAMSM: from 07/06/2007 to 13/06/2007 each of
>> 00,03,06,09,12,15,18 and 21 UTC
>
> Summer experiment 2: period of MSM-DA: from 00 UTC 30/06/2007 to 21 UTC 15/07/2007
>> period of JMAMSM: from 01/07/2007 to 15/07/2007 each of
>> 00,03,06,09,12,15,18 and 21 UTC
>
> Winter   experimet : period of MSM-DA: from 00 UTC 25/12/2006 to 21 UTC 31/12/2006
>> period of JMAMSM: from 25/12/2006 to 31/12/2006 each of
>> 00,03,06,09,12,15,18 and 21 UTC

> CNTL)   with SATOB AMVs from MTSAT-1R (identical to the operational data)
>> ➢ Using the quality control procedure before the revision (The details are section 3.)
>
> THIN_200KM) with BUFR AMVs generated from MTSAT-1R (including hourly AMVs) satellite
>> ➢ Using the revised quality control procedure (The details are section 3.)
>> ➢ Use in every 2 deg. by 2 deg. thinning box in six-hour time windows
>> ➢ Almost same as TEST of GSM-DA version
>
> THIN_100KM) with BUFR AMVs generated from MTSAT-1R (including hourly AMVs) satellite
>> ➢ Using the revised quality control procedure (The details are section 3.)
>> ➢ Use in every 1 deg. by 1 deg. thinning box in six-hour time windows
>
> THIN_200KM_EACH) with BUFR AMVs generated from MTSAT-1R (including hourly AMVs) satellite
>> ➢ Using the revised quality control procedure (The details are section 3.)
>> ➢ Use in every 2 deg. by 2 deg. thinning box in each of six-hour time windows

5. RESULTS

(A) RESULTS FOR GSM-DA

Figure 6 shows U-component wind speed biases verified against radiosonde observations in January 2006. TEST is nearer to zero than CNTL in analysis and first guess. It means that the new AMV scheme reduced the slow bias of wind speed in analysis fields in GSM-DA. Especially, wind speed biases at upper level over 500 hPa are significantly reduced. RMSE of wind speed in analysis fields were slightly smaller or neutral (not shown). These characteristics are also shown in summer experiments, in September 2005. Figure 7 shows forecast improvement rate with respect to RMSE for 1-9 day forecasts in winter experiments. The horizontal axis is forecast hours and the vertical axis the rate of improvement, which is calculated with the next formula.

$$\frac{\left(RMSE_{CNTL} - RMSE_{TEST}\right)}{RMSE_{CNTL}} \quad (2)$$

Figure 7 shows many positive values or large improvement. In particular there is a clear improvement in two-day forecast ability in terms of 250 hPa winds, 500 hPa geopotential heights and 850 hPa temperatures mainly in the southern hemisphere for GSM-DA. Results of summer experiment are slightly positive or neutral on forecast. The result of tropics in terms of 500 hPa geopotential heights looks statistically significantly worse. This reason is as follows. Our forecast model has negative biases of temperature in the lower troposphere. Analyzed temperature in TEST tends to be warmer in the mid and low troposphere compared to CNTL. As temperature biases of forecast model contradict analyzed temperature, forecast errors of temperature become large. We think that these effects could worsen the 500 hPa geopotential heights in the forecast improvement rate. But differences of the 500 hPa geopotential heights between TEST and CNTL are small.

Figure 8 shows averaged typhoon track error in September 2005. TEST shows slightly better typhoon track forecast.

(B) RESULTS FOR MSM-DA

Figure 9 shows RMSEs and biases of forecasts at initial times verified against winds speeds of Japanese radiosonde observations from 1 to 15 July 2007. RMSE and biases for wind against radiosonde observations in each scheme are smaller than CNTL. Especially THIN_200KM or THIN_200KM_EACH reduce the slow bias and RMSE of wind speed in analysis fields compared to radiosonde observations. These characteristics are also shown in others periods.

Figure 10 shows threat scores against Radar-AMeDAS composite precipitation data in Japan (R/A) from 1 to 15 July 2007. The left panel is threat score for each threshold of precipitation. The right panel is threat score for each forecast time of 20 mm per 3 hours of precipitation. Resolution of this verification is in 20 km grid. There is a slight improvement in the THIN_200KM scheme in one-day forecast for precipitation over 15 mm per three hours around Japan. The results of other experiment periods were
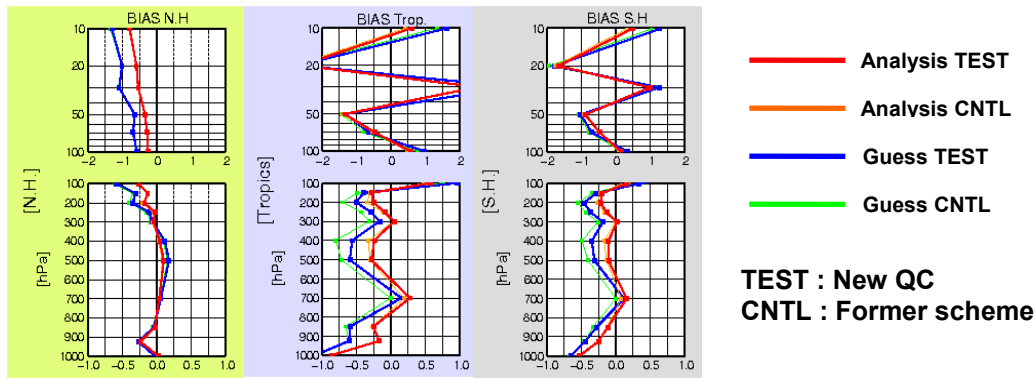
Figure 6: U-component wind speed biases against radiosonde observations in January 2006.
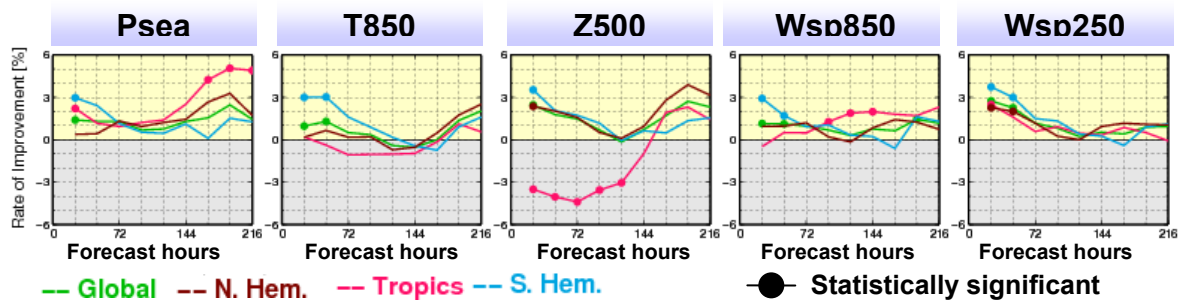
Figure 7: Forecast Improvement Rate wrt RMSE for 1-9 day forecasts in January 2006. "Psea" is surface pressure. "T850" is 850 hPa temperatures. "Z500" is 500 hPa geopotential heights. "Wsp850" is 850 hPa wind speeds. "Wsp250 " is 250 hPa wind speeds.
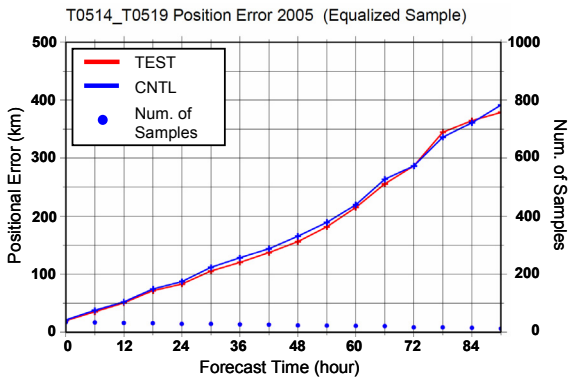
Figure 8: Averaged typhoon track error in September 2005 (citation from Yamashita, 2007). Blue dots indicate the number of cases used in this statistics. "TEST" is New QC. "CNTL" is Former sheme.

similar to the results of this experiment.

Fig 9 and 10 show that THIN_100KM scheme does not give improvement over other schemes and it may reflect spatial correlation of observation errors.

6. TOPICS

In the section 5(B), we found the interesting results. Figure 11 is threat scores for each threshold of precipitation in Kyushu and Chubu areas from 1 to 15 July 2007. THIN_100KM of threat score in Kyushu area shows the highest value, while that in Chubu area shows the lowest value. This good result in Kyushu shows a possibility that the thinning interval of AMVs can be reduced from 200 km or 2 degrees in horizontal to bring good impacts on forecast. In this experimental period, there was a stationary front lying in Kyushu and many AMVs were generated in Kyushu compared to Chubu. So, we will try to perform this validation experiment, selecting area including many AMVs. On the other hand, the result in Chubu may show the bad effect of spatial correlation of observation errors. We are investigating this cause.

7. CONCLUSION
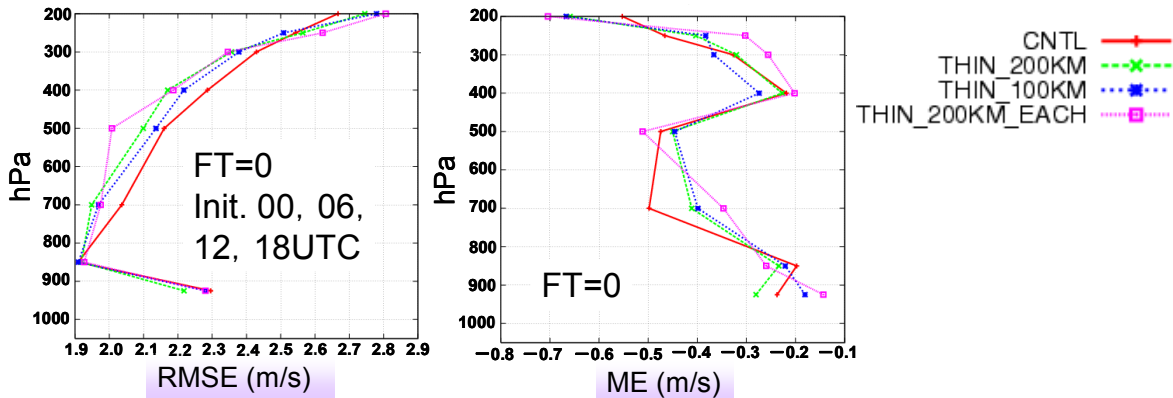
Figure 9: RMSE of AMVs (left side figure) and ME of AMVs (right side figure) against Japan Radiosonde Wind speeds from 1 to 15 July 2007. "FT" is Forecast time. "Init" is initial forecast time. "ME" is mean error (bias).
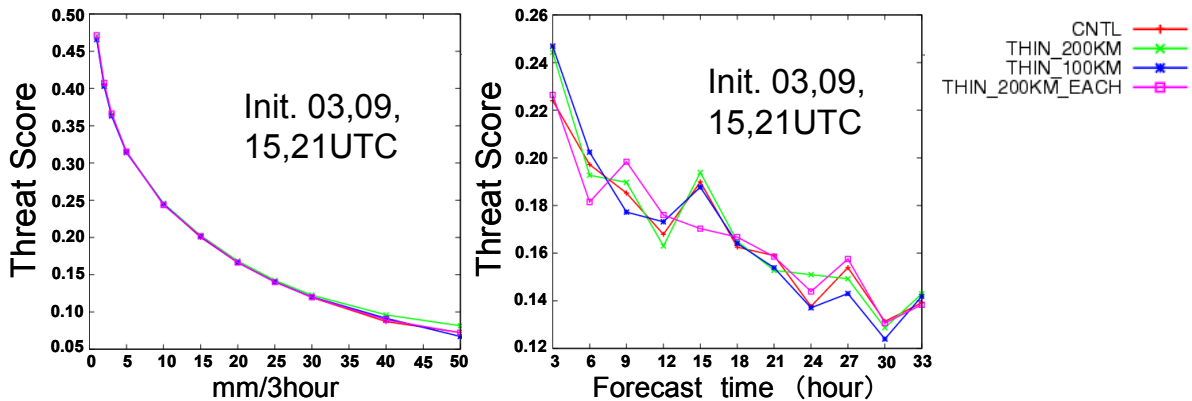
Figure 10: Threat score against R/A from 1 to 15 July 2007. Left side figure is threat score for each threshold of precipitation. Right side figure is threat score for each forecast time of 20 mm per 3 hours of precipitation. "Init" is initial forecast time.
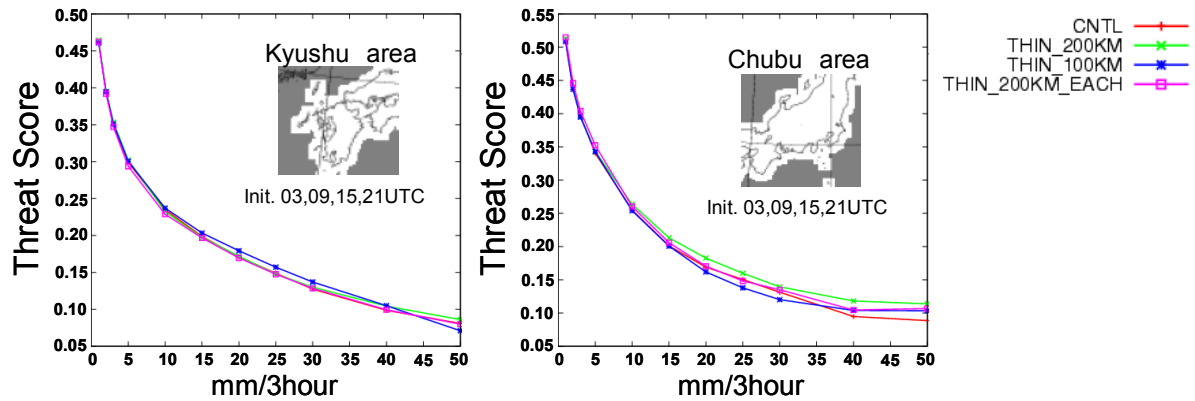
Figure 11: Threat score for each threshold of precipitation against R/A from 1 to 15 July 2007. Left side figure is threat score for Kyushu area. Right side figure is threat score for Chubu area. "Init" is initial forecast time.

The usage of AMVs in the BUFR AMVs generated from all geostationary satellites was revised in the JMA operational GSM-DA on 18 October 2006 and in the JMA operational MSM-DA on 7 December 2007. The revisions are adding hourly MTSAT-1R AMVs, more reasonable blacklist, stricter and finer QI screening and upgraded thinning scheme. The new AMV scheme reduced the slow bias and RMSE of wind speed in analysis fields compared to radiosonde measurements in both the assimilation systems. It also improved two-day forecast ability in terms of 250 hPa winds, 500 hPa geopotential heights and 850 hPa temperatures mainly in the southern hemisphere for GSM-DA. In the MSM-DA with new AMV scheme, there was an improvement in one-day forecasting for precipitation over 15 mm per three hours around Japan.

We also got a possibility that the thinning interval of AMVs can be reduced from 200 km or 2 degrees in horizontal to bring good impacts on forecast.

8.   REFERENCES

Hollingsworth, A., and P. Lönnberg, (1986) The statistical structure of short-range forecast errors as determined from radiosonde data. Part I: The wind field. Tellus, 38A, pp 111-136.

Imai, T., (2006) Status of atmospheric motion vector in JMA, *Proceedings of 8th IWW*, China.

Kazumori, M. and Y., Nakamura, (2004) MODIS polar winds assimilation experiments at JMA., *Proceedings of 7th IWW*, Finland.

Nakamura, Y., E., Ozawa, K., Onogi and R., Kumabe., (2002) Impact experiments on NWP with rapid scan AMVs, *Proceedings of 6th IWW*, pp 171-189.

Sato, Y. and R. Kumabe, (2004) A case study of hourly AMV assimilation with JMA-MSM, *Proceedings of 7th IWW*, Finland.

Yamashita, K., (2006) Assimilation of Hourly MTSAT-1R AMV into JMA-MSM, *Proceedings of 8th IWW*, China.

Yamashita, K., (2007) Revised usage of Atmospheric Motion Vectors (AMV) from all geostationary satellites in the operational global 4D-Var assimilation system., CAS/JAC WGNE Research Activities in Atmospheric and Oceanic Modelling, 37, pp 26.